

# Formation of a Bridging Phosphinidene Thorium Complex

Andrew C. Behrle,<sup>†</sup> Ludovic Castro,<sup>‡</sup> Laurent Maron,<sup>\*,‡</sup> and Justin R. Walensky<sup>\*,†</sup>

<sup>†</sup>Department of Chemistry, University of Missouri, Columbia, Missouri 65211, United States

<sup>‡</sup>Universite de Toulouse and CNRS, INSA, UPS, CNRS, UMR, UMR 5215, LPCNO, 135 Avenue de Rangueil, F-31077 Toulouse, France

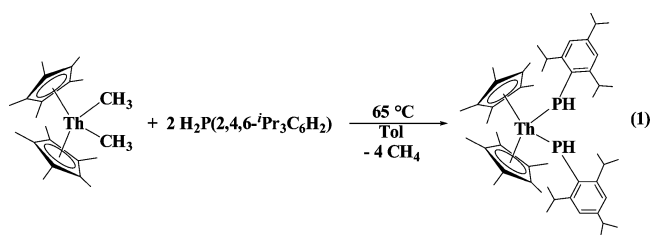
**S** Supporting Information

**ABSTRACT:** The synthesis and structural determination of the first thorium phosphinidene complex are reported. The reaction of 2 equiv of  $(C_5Me_5)_2Th(CH_3)_2$  with  $H_2P(2,4,6-iPr_3C_6H_2)$  at  $95\text{ }^\circ\text{C}$  produces  $[(C_5Me_5)_2Th]_2(\mu_2-P[(2,6-CH_2CHCH_3)_2-4-iPrC_6H_2])$  as well as 4 equiv of methane, 2 equiv from deprotonation of the phosphine and 2 equiv from C–H bond activation of one methyl group of each of the isopropyl groups at the 2- and 6-positions. Transition state calculations indicate that the steps in the mechanism are P–H, C–H, C–H, and then P–H bond activation to form the phosphinidene.

Despite the fact that it is isoelectronic with the imido functional group,  $[=NR]^{2-}$ , there is a paucity of complexes bearing the phosphinidene moiety,  $[=PR]^{2-}$ .<sup>1–4</sup> This is especially true in the case of f elements.<sup>5–8</sup> The isolation of metal phosphinidene complexes is attractive, as they have been invoked in catalytic reactions<sup>1</sup> and can be used to examine the molecular and electronic structure of metal–ligand multiple bonding<sup>2</sup> as well as to advance the fundamental chemistry of actinides coupled with the understudied area of actinide–phosphorus bonds.

Our group has been interested in examining the structure, bonding, and reactivity of actinides with soft donor ligands such as sulfur and selenium.<sup>9</sup> We produced a series of eight-coordinate homoleptic complexes that showed little reaction chemistry. For the pnictogen group, there are no homoleptic complexes bearing phosphorus, and thus, we turned to the ubiquitous metallocene ligand platform  $[(C_5Me_5)_2Th]^{2+}$ . There are approximately 17 structures with actinide–phosphorus bonds containing an anionic phosphorus ligand.<sup>5,7,8,10–17</sup> Only four of these contain the phosphinidene ( $PR^{2-}$ ) moiety. Because of the highly debated covalent nature of actinide–ligand bonding and the rarity of these complexes with actinides, our objective was to investigate actinide–phosphorus compounds.

The reaction of  $H_2P(2,4,6-iPr_3C_6H_2)$  with  $(C_5Me_5)_2Th(CH_3)_2$  in 1:1 and 2:1 stoichiometric ratios led to the formation of  $(C_5Me_5)_2Th[PH(2,4,6-iPr_3C_6H_2)]_2$  (**1**) (eq 1). Complex **1** has a  $^{31}P\{^1H\}$  resonance at 1.66 ppm. This is in contrast to the  $^{31}P\{^1H\}$  resonances for  $(C_5Me_5)_2Th(PR_2)_2$ , which appear at 144, 136, and 205 ppm for R = Ph, Et, and Cy, respectively. Hence, the substituents on phosphorus make a significant difference in the shift of the  $^{31}P$  NMR resonance. In the P:Th = 1:1 reaction, compound **1** is formed along with a



dehydrocoupled phosphine product as the byproduct, but this is not  $(2,4,6-iPr_3C_6H_2)_2(PH)_2$  on the basis of  $^{31}P$  NMR spectroscopy.<sup>18</sup> The dehydrocoupled product is unknown. In both cases, heating to at least  $65\text{ }^\circ\text{C}$  is required for reaction shown in eq 1 to occur. Complex **1**, which has a vibrant orange color, is a rare example of a primary phosphido complex with any actinide and the first with thorium. Its structure is shown in Figure 1.

However, when 2 equiv of  $(C_5Me_5)_2Th(CH_3)_2$  was reacted with 1 equiv of  $H_2P(2,4,6-iPr_3C_6H_2)$  at  $95\text{ }^\circ\text{C}$  for 12 h in toluene (eq 2), a red-orange product with an  $^1H$  NMR spectrum exhibiting two distinct  $C_5Me_5^-$  resonances was

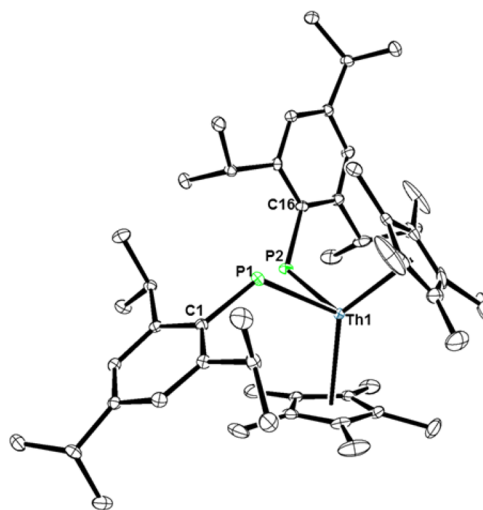
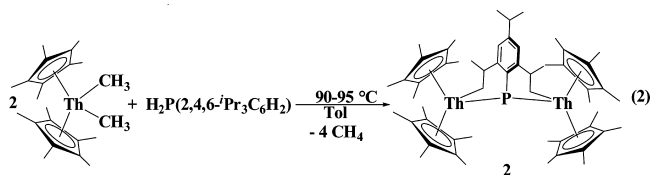


**Figure 1.** Thermal ellipsoid plot of **1** shown at the 50% probability level. Hydrogen atoms have been omitted for clarity. Selected bond distances (Å) and angles (deg): Th1–P1, 2.8754(6); Th1–P2, 2.8830(6); P1–C1, 1.842(2); P2–C16, 1.843(2); P1–Th1–P2, 92.180(18); Th1–P1–C1, 121.26(7); Th1–P2–C16, 121.91(7).

Received: September 18, 2015

Published: November 17, 2015



obtained, and only one phosphorus product was observed in the  $^{31}\text{P}\{^1\text{H}\}$  NMR spectrum. Interestingly, this  $^{31}\text{P}$  signal was located far downfield at 161.9 ppm. Only a singlet was observed in the proton-coupled experiment, and no P–H stretching frequency was seen in the IR spectrum; hence, this resonance corresponded to a phosphorus atom without a coordinated proton. This is the region of the  $^{31}\text{P}$  NMR resonance for a bridging phosphinidene lutetium complex.<sup>6</sup> The structure was determined by X-ray crystallography to be  $[(\text{C}_5\text{Me}_5)_2\text{Th}]_2(\mu_2\text{-P}[(2,6\text{-CH}_2\text{CHCH}_3)_2\text{-4-}i\text{PrC}_6\text{H}_2])$  (**2**) (Figure 2). Complex **2** is the first structurally determined phosphinidene complex with thorium that has been reported and only the fifth with an actinide overall.

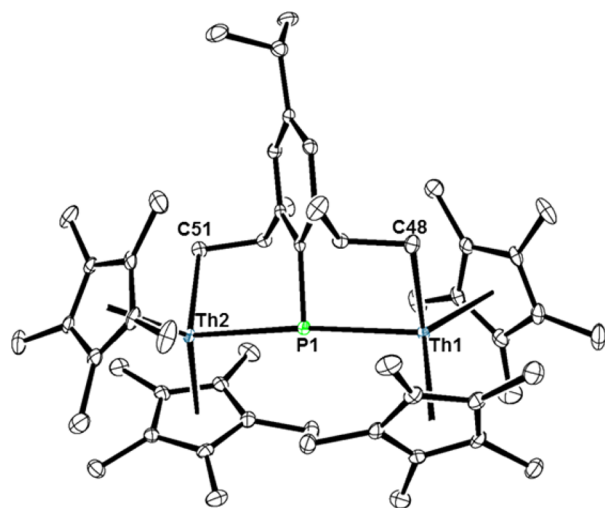


**Figure 2.** Thermal ellipsoid plot of **2** shown at the 50% probability level. Hydrogen atoms have been omitted for clarity. Selected bond distances (Å) and angles (deg): Th1–P1, 2.8083(9); Th1–C48, 2.482(3); Th2–P1, 2.8186(9); Th2–C51, 2.472(3); Th1–P1–Th2, 173.99(3); P1–Th2–C51, 95.19(8).

Complex **2** is the result of two P–H bond activations as well as two C–H bond activations to give each thorium center two  $\text{C}_5\text{Me}_5^-$  ligands, one Th–C bond, and one Th–P bond. The presence of two  $\text{C}_5\text{Me}_5^-$  resonances in the  $^1\text{H}$  NMR spectrum is presumably due to the steric congestion about the thorium center, which restricts the rotation of the  $\text{C}_5\text{Me}_5^-$  ligands. The Th–C bond distances of 2.482(3) and 2.472(3) Å are shorter than the distances of 2.551(7) and 2.552(7) Å observed in  $(\text{C}_5\text{Me}_5)_2\text{Th}(\text{CH}_2\text{Ph})_2$ .<sup>19</sup> Since the phosphinidene is bridging, the Th–P bond lengths are only slightly shorter than in **1**: the Th–P bond lengths in **1** are 2.8755(6) and 2.8829(7) Å, while Th–P bond lengths of 2.8083(9) and 2.8186(9) Å are observed in **2**. One interesting feature of **2** is the nearly linear Th–P–Th bond angle of  $173.99(3)^\circ$ , which is much larger than the angle of  $157.7(2)^\circ$  seen in Marks'  $[(\text{C}_5\text{Me}_5)_2(\text{OCH}_3)\text{U}]_2(\mu_2\text{-PH})$  complex.<sup>8</sup> This is due to the Th– $\text{CH}_2$  linkages which enforce the linearity of the Th–P–Th bond angle as well as a planar

phosphorus geometry with a Th1–P1–C41 (ipso carbon) bond angle of  $93.81(10)^\circ$ .<sup>20</sup>

The bonding in **2** was interrogated using density functional theory (DFT) calculations. Natural bond orbital (NBO) analysis showed that there is no Th–P multiple-bonding character, and two polar covalent bonds with 80% P and 20% Th character are observed (Figure 3).

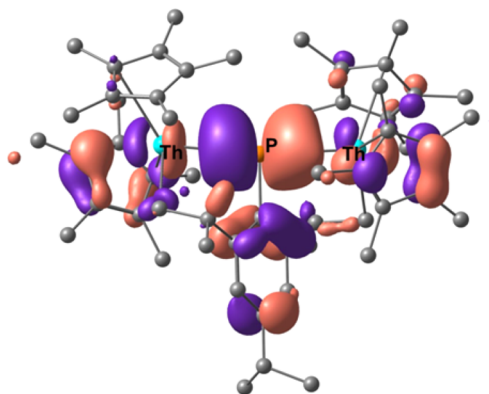


**Figure 3.** Plot of the HOMO–1 displaying the interaction between P and the two Th centers.

A proposed mechanism for the formation of **2** was also studied theoretically using DFT calculations (Figure 4). The first transition state, **TS1**, corresponds to P–H activation of the phosphine. The proton is transferred from phosphorus to a methyl ligand of the thorium complex to give **Int1** with the concomitant release of a methane molecule. The optimized three-dimensional (3D) structures of **TS1** and **Int1** are reported in Figure S6. The substrate does not bind between the two methyl groups in order to avoid steric repulsions between its  $i\text{Pr}$  groups and the methyl substituents of the cyclopentadienyl ligands on thorium. **TS1**, like the other transition states found (**TS2**, **TS3**, and **TS4**), is a classic four-center  $\sigma$ -bond metathesis transition state, with P, H, and C almost aligned ( $172.5^\circ$ ). The activation barrier was calculated to be +23.4 kcal/mol, so the reaction is kinetically accessible. This can be explained by the favorable charge alternation (calculated with the natural population analysis (NPA) technique) at the transition state level: +2.20 for Th, –0.24 for P, +0.03 for H, and –0.49 for  $\text{CH}_3$ . Moreover, there is a stabilizing  $\alpha$ -agostic interaction between a C–H bond of  $\text{CH}_3$  and Th. Once the methane molecule is released, the complex relaxes to give **Int1**, whose formation is thermodynamically favored (–11.3 kcal/mol). The Th–P bond is formed (2.90 Å) while the Th–P–H angle is quite tight ( $105.8^\circ$ ), but these compare well with the Th–P bond distance of 2.8829(7) Å and Th1–P1–H1 angle of  $106.5^\circ$  in **1**.

The second transition state, **TS2**, corresponds to the subsequent C–H activation of one of the  $\text{sp}^3$  carbons of the  $i\text{Pr}$  group at the ortho position of the phenyl substituent. The proton is transferred to the remaining methyl ligand of the thorium complex, leading to the formation of **Int2** and the release of another methane molecule. The optimized 3D structures of **TS2** and **Int2** are presented in Figure S7. The relative activation barrier was calculated to be +30.8 kcal/mol. Thus, this reaction is kinetically accessible but definitely slower than the first step. The explanation for that higher barrier is that the proton of the  $\text{sp}^3$  carbon of  $i\text{Pr}$  is less acidic than the proton

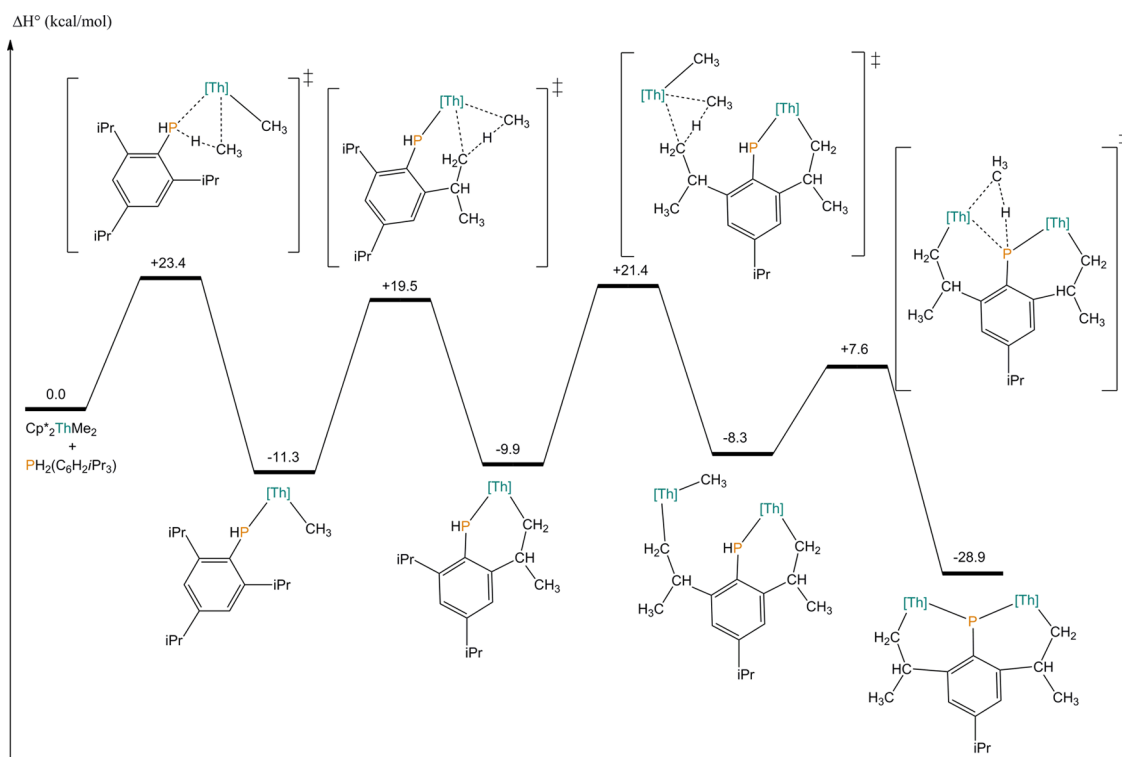


**Figure 4.** Calculated energy profile of the reaction of  $(C_5Me_5)_2Th(CH_3)_2$  with  $H_2P(2,4,6-iPr_3C_6H_2)$ . For clarity, [Th] represents  $(C_5Me_5)_2Th$ .

of the phosphine group. This reaction step is almost athermic (+1.4 kcal/mol with respect to **Int2**).

The formation of a terminal phosphinidene was also calculated (Figure S8). In order to transfer a proton to the remaining methyl ligand, the hydrogen has to be oriented toward the alkyl prior to the transition state level. Thus, a rotation of the  $[PH(^iPr_3C_6H_2)]^-$  ligand must be performed after the first step of the reaction. This process is sterically demanding since it involves strong repulsion between the  $iPr$  groups and the  $Cp^*$  ligands. The subsequent proton transfer is kinetically facile but thermodynamically not favorable. Thus, the  $(C_5Me_5)_2Th=P(^iPr_3C_6H_2)$  product is less stable than the previous intermediate and should not be observed. The only possible reaction after the first P–H activation is thus the C–H activation of the  $iPr$  group.

The third transition state, **TS3**, corresponds to the C–H activation of one of the  $sp^3$  carbons of the other  $iPr$  group at the ortho position of the phenyl substituent by another thorium complex. Even though the P–H bond is more acidic than this C–H bond, the P–H activation cannot be carried out yet because of strong steric hindrance. Once again, the  $iPr$  group does not come between the two methyl groups in order to avoid steric repulsions between the phenyl substituent and the methyl substituents of the  $Cp$  group. The proton is transferred to a methyl group to form **Int3** with concomitant release of a methane molecule. The optimized 3D structures of **TS3** and **Int3** are presented in Figure S9. The relative activation barrier was calculated to be +31.3 kcal/mol. The charge alternation of the transition state is still very good (+2.32 for Th, –0.41 for  $CH_2$ , +0.21 for H, and –0.41 for  $CH_3$ ), but the poor acidity of the methyl group of  $iPr$  leads to a quite high activation barrier. This reaction step is almost athermic (+1.6 kcal/mol with respect to **Int2**). In **Int2**, the phosphorus atom interacts with both Th centers (3.05 and 3.36 Å). As a consequence, the  $CH_3-Th-CH_2$  angle of the new thorium complex is very large

(134.9°), and the methyl ligand is in ideal position for the next step of the reaction, namely, the P–H activation.

The fourth transition state, **TS4**, corresponds to the P–H activation leading to the formation of the final product of the reaction and another methane molecule. The proton is transferred to the last methyl group of the second thorium complex. The optimized 3D structures of **TS4** and **Prod** are presented in Figure S10. The P–H bond and methyl groups are both perfectly oriented in **Int3** to form **TS4**, with P, H, and  $CH_3$  slightly less aligned than for the previous transition states (160.6°) because of the lack of flexibility of the bimetallic complex. The relative activation barrier was calculated to be +15.9 kcal/mol, indicating that this step is kinetically very accessible. This is due to both the high acidity of the P–H group and the convenient orientation of the reacting groups in **Int3**. The charge alternation at the transition state level is also very good: +2.20 for Th, –0.25 for P, +0.10 for H, and –0.46 for  $CH_3$ . Moreover, this last step is thermodynamically very favorable (–20.6 kcal/mol with respect to **Int3**). The comparison between the optimized and experimental geometrical parameters of **Prod** is reported in Table S2. There is very good agreement between the computed and observed structures. The calculated Th–P distances are slightly longer because of the use of the 5f-in-core pseudopotential for thorium. However, it is now well-documented that the use of 5f-in-core pseudopotentials for actinides leads to slightly overestimated activation barriers, so the reaction should be kinetically accessible experimentally.<sup>21,22</sup> Globally, the reaction is thermodynamically very favorable (–28.9 kcal/mol) but somewhat difficult kinetically because of the C–H activations of the  $sp^3$  carbons of the  $iPr$  groups (~30 kcal/mol), in very good agreement with the experimental conditions.

The reactivity of **2** was probed with elemental sulfur and  $CS_2$  for possible insertion into the Th–C bond as well as  $HO(2,6-Me_2C_6H_3)$  and  $HPPH_2$  to add via protonation of the Th–C

bonds. Efforts were further made to oxidize the P(III) to P(V) using *N*-morpholine oxide. None of the insertion or oxidation reactions were successful. Protonation using HO(2,6-Me<sub>2</sub>C<sub>6</sub>H<sub>3</sub>) produced (C<sub>5</sub>Me<sub>5</sub>)<sub>2</sub>Th[O(2,6-Me<sub>2</sub>C<sub>6</sub>H<sub>3</sub>)<sub>2</sub>] (3) (Figure S5), H<sub>2</sub>P(2,4,6-<sup>i</sup>Pr<sub>3</sub>C<sub>6</sub>H<sub>2</sub>), unreacted 2, and an unidentified phosphorus product. The reaction of 1 with 2 equiv of HO(2,6-Me<sub>2</sub>C<sub>6</sub>H<sub>3</sub>) also produces 3 and H<sub>2</sub>P(2,4,6-<sup>i</sup>Pr<sub>3</sub>C<sub>6</sub>H<sub>2</sub>). No reaction between 2 and HPPH<sub>2</sub> was observed, even upon heating to 95 °C for 12 h. Even a reagent such as benzophenone, which might have been expected to exhibit Wittig-type reactivity, failed to produce any reaction. The inertness of 2 is presumably due to its six-membered metallocycle. Furthermore, the weak nature of the Th–P bond leads to ligand redistribution and uncontrollable protonation. The inability of the phosphorus to undergo oxidation may be the result of an inductive effect from the two thorium cations or steric encumbrance provided by the pentamethylcyclopentadienyl ligands.

In summary, a thorium phosphinidene complex obtained from the reaction of 2 equiv of (C<sub>5</sub>Me<sub>5</sub>)<sub>2</sub>Th(CH<sub>3</sub>)<sub>2</sub> with H<sub>2</sub>P(2,4,6-<sup>i</sup>Pr<sub>3</sub>C<sub>6</sub>H<sub>2</sub>) has been reported. This reaction produces a bridging phosphinidene with two concomitant C–H bond activations. This represents the first structural characterization of a thorium phosphinidene and a rare example of such a complex with an actinide. Additionally, a rare bis(phosphido) and first primary phosphido complex with thorium has been isolated. This demonstrates the ability of thorium to act as a strong Lewis acid and the novel chemistry that can exist with actinide–pnictogen bonds.

## ■ ASSOCIATED CONTENT

### 📄 Supporting Information

The Supporting Information is available free of charge on the ACS Publications website at DOI: 10.1021/jacs.5b09826.

Experimental, crystallographic, and computational details (PDF)

Crystallographic data for 1, 2, and 3 (CIF)

## ■ AUTHOR INFORMATION

### Corresponding Authors

\*walenskyj@missouri.edu

\*laurent.maron@irsamc.ups-tlse.fr

### Notes

The authors declare no competing financial interest.

## ■ ACKNOWLEDGMENTS

J.R.W. gratefully acknowledges support for this work from the U.S. Department of Energy, Office of Science, Early Career Research Program under Award DE-SC-0014174. L.M. thanks the Humboldt Foundation, and CalMip is acknowledged for a grant of computing time.

## ■ REFERENCES

- (1) Ehlers, A. W.; Baerends, E. J.; Lammertsma, K. *J. Am. Chem. Soc.* **2002**, *124*, 2831.
- (2) Aktaş, H.; Slootweg, J. C.; Lammertsma, K. *Angew. Chem., Int. Ed.* **2010**, *49*, 2070.
- (3) Waterman, R. *Dalton Trans.* **2009**, 18.
- (4) Hayton, T. W. *Chem. Commun.* **2013**, *49*, 2956.
- (5) Gardner, B. M.; Balázs, G.; Scheer, M.; Tuna, F.; McInnes, E. J. L.; McMaster, J.; Lewis, W.; Blake, A. J.; Liddle, S. T. *Angew. Chem., Int. Ed.* **2014**, *53*, 4484.

(6) Masuda, J. D.; Jantunen, K. C.; Ozerov, O. V.; Noonan, K. J. T.; Gates, D. P.; Scott, B. L.; Kiplinger, J. L. *J. Am. Chem. Soc.* **2008**, *130*, 2408.

(7) Arney, D. S. J.; Schnabel, R. C.; Scott, B. C.; Burns, C. J. *J. Am. Chem. Soc.* **1996**, *118*, 6780.

(8) Duttera, M. R.; Day, V. W.; Marks, T. J. *J. Am. Chem. Soc.* **1984**, *106*, 2907.

(9) Behrle, A. C.; Barnes, C. L.; Kaltsoyannis, N.; Walensky, J. R. *Inorg. Chem.* **2013**, *52*, 10623.

(10) Patel, D.; Tuna, F.; McInnes, E. J. L.; Lewis, W.; Blake, A. J.; Liddle, S. T. *Angew. Chem., Int. Ed.* **2013**, *52*, 13334.

(11) Tsoureas, N.; Kilpatrick, A. F. R.; Summerscales, O. T.; Nixon, J. F.; Cloke, F. G. N.; Hitchcock, P. B. *Eur. J. Inorg. Chem.* **2013**, *2013*, 4085.

(12) Frey, A. S. P.; Cloke, F. G. N.; Hitchcock, P. B.; Green, J. C. *New J. Chem.* **2011**, *35*, 2022.

(13) Scherer, O. J.; Werner, B.; Heckmann, G.; Wolmershäuser, G. *Angew. Chem., Int. Ed. Engl.* **1991**, *30*, 553.

(14) Hall, S. W.; Huffman, J. C.; Miller, M. M.; Avens, L. R.; Burns, C. J.; Sattelberger, A. P.; Arney, D. S. J.; England, A. F. *Organometallics* **1993**, *12*, 752.

(15) Hay, P. J.; Ryan, R. R.; Salazar, K. V.; Wroblewski, D. A.; Sattelberger, A. P. *J. Am. Chem. Soc.* **1986**, *108*, 313.

(16) Wroblewski, D. A.; Ryan, R. R.; Wasserman, H. J.; Salazar, K. V.; Paine, R. T.; Moody, D. C. *Organometallics* **1986**, *5*, 90.

(17) Ritchey, J. M.; Zozulin, A. J.; Wroblewski, D. A.; Ryan, R. R.; Wasserman, H. J.; Moody, D. C.; Paine, R. T. *J. Am. Chem. Soc.* **1985**, *107*, 501.

(18) Zou, J.; Berg, D. J.; Oliver, A.; Twamley, B. *Organometallics* **2013**, *32*, 6532.

(19) Jantunen, K. C.; Burns, C. J.; Castro-Rodriguez, I.; Da Re, R. E.; Golden, J. T.; Morris, D. E.; Scott, B. L.; Taw, F. L.; Kiplinger, J. L. *Organometallics* **2004**, *23*, 4682.

(20) Dunn, N. L.; Ha, M.; Radosevich, A. T. *J. Am. Chem. Soc.* **2012**, *134*, 11330.

(21) Castro, L.; Yahia, A.; Maron, L. *ChemPhysChem* **2010**, *11*, 990.

(22) Castro, L.; Yahia, A.; Maron, L. *Dalton Trans.* **2010**, *39*, 6682.